Isoscalar spin strength in ^{12}C measured in 400 MeV deuteron inelastic scattering

B. N. Johnson,[1,2] M. Morlet,[1] C. Djalali,[1,2] F. T. Baker,[3] L. Bimbot,[1]
C. Glashausser,[4] J. Guillot,[1] H. Langevin-Joliot,[1] N. Marty,[1]
L. Rosier,[1] E. Tomasi-Gustafsson,[5] J. Van de Wiele,[1] and A. Willis[1]
[1] *CNRS-IN2P3, Institut de Physique Nucléaire, Orsay, BP No. 1, 91406, France*
[2] *Department of Physics and Astronomy, University of South Carolina, Columbia, South Carolina 29208*
[3] *Department of Physics and Astronomy, University of Georgia, Athens, Georgia 30602*
[4] *Department of Physics and Astronomy, Rutgers University, New Brunswick, New Jersey 08903*
[5] *DAPNIA-SPhN and Laboratoire National Saturne, CEN Saclay, 91191 Gif-sur-Yvette CEDEX, France*
(Received 7 December 1994)

The isoscalar spin strength in ^{12}C has been studied in the inelastic scattering of polarized 400 MeV deuterons. The measurements were carried out over an angular range from 3° to 7° and an excitation energy range from 11 to 58 MeV (momentum transfer range from 0.34 to 0.92 fm^{-1}). Previously unknown spin excitations were found in the 20-MeV region and over a broad range in the continuum with a cluster of strength around 30 MeV. The results are compared with spin-flip probability measurements in proton scattering. Below 35 MeV of excitation energy, the isoscalar relative spin response is strongly enhanced above the noninteracting Fermi gas value of 0.5. Above 35 MeV of excitation the spin response drops below 0.5.

PACS number(s): 25.45.De, 21.10.Hw, 27.20.+n

I. INTRODUCTION

The study of spin degrees of freedom in nuclei has been an area of intense activity and interest, both theoretical and experimental, since the beginning of the past decade. Nuclear spin excitations have been induced and studied via a number of different reactions. Charge exchange reactions such as (p,n) and (^{3}He,t) are purely isovector in nature and have successfully located isovector dipole and quadrupole spin strength in many nuclei [1–4]. Spin excitations have also been measured both by electron [5] and proton inelastic scattering [6–11]. The $(\vec{p},\vec{p}')$ experiments [8–11] have successfully localized spin dipole and quadrupole strength in several nuclei. The electromagnetic interaction excites both isospin channels, but the isoscalar spin component is suppressed relative to the isovector one by at least an order of magnitude. Inelastic proton scattering also excites both isospin channels, and again the isoscalar spin-flip cross sections are generally significantly smaller than the isovector ones. As a result, very few isoscalar spin states are presently known and the isoscalar spin strength in the continuum has remained essentially unexplored.

Recent work has demonstrated that $(\vec{d},\vec{d}')$ scattering at 400 MeV is an efficient tool for isolating the isoscalar spin channel in the nuclear excitation spectrum. A reliable signature (S_d^y) for isoscalar spin-flip transitions was developed and tested on low-lying levels in ^{12}C [12]. This signature was first used to measure the isoscalar spin response in ^{40}Ca, for excitation energies up to 42 MeV [13]. These results were combined with the $(\vec{p},\vec{p}')$ data taken at similar momentum transfers on ^{40}Ca in order to resolve the total spin response into its separate isospin components.

The current work represents the second experiment in an ongoing program in which $(\vec{d},\vec{d}')$ scattering is used to map out isoscalar spin strength in the continuum. The initial tests of the signature on ^{12}C suggested the possibility of significant ΔS=1, ΔT=0 strength above 20 MeV of excitation energy [12]. Measurements were performed for excitation energies ranging from 11 to 58 MeV and for angles between 3° and 7° (momentum transfer q between 0.34 and 0.92 fm^{-1}). The present results are compared to the total spin strength observed in $(\vec{p},\vec{p}')$ scattering [14]. In Sec. II expressions for the spin observables that were derived in Ref. [12] are given and the effect of distortion on the signature is discussed. Section III contains a brief description of the experimental set-up and the procedure that was followed to extract the spin observables. The experimental results are given and discussed in Sec. IV; the summary and conclusions are presented in Sec. V.

II. SIGNATURE FOR SPIN-FLIP TRANSITIONS

A. Description of the signature

The $(\vec{p},\vec{p}')$ studies [8–11] were carried out by measuring, as a function of excitation energy, the quantity S_{nn}, which is close to zero for ΔS=0 states but is generally large for spin transitions. The quantity S_{nn} is the probability that the proton undergoes a spin-flip during the reaction. For a deuteron beam, three spin-flip probabilities S_0, S_1, and S_2 may be defined; they are the probabilities for a change of 0, 1, or 2 units of the spin projection along the y axis, which is taken perpendicular to the reaction plane. The expressions for all these probabilities are given in Refs. [12,13]. Only the S_1 probability, which is analogous to S_{nn} in $(\vec{p},\vec{p}')$ scattering, will be given here:

$$S_1 = \tfrac{1}{9}(4 - A^{yy} - P^{y'y'} - 2K^{y'y'}_{yy}). \quad (2.1)$$

Following the Madison convention [15] and the formalism of Ref. [16], A_y and A_{yy} are the vector and tensor analyzing powers of the reaction, $P^{y'}$ and $P^{y'y'}$ the vector and tensor polarizing powers of the reaction, and $K^{y'}_y$ and $K^{y'y'}_{yy}$ the vector and tensor polarization transfer coefficients. The lower indices refer to the incoming beam, and the upper, primed indices to the outgoing beam.

It has been shown [16] that, in the plane wave approximation, S_1=0 for ΔS=0 transitions. For ΔS=1 transitions S_1 should be different from zero. The quantity S_1, however, is not so readily measured as S_{nn}, since one needs to measure the tensor polarization of the scattered deuteron, a difficult measurement requiring a suitable tensor polarimeter. We can get around this difficulty by considering the observable $S^y_d = S_1 + 4S_2 + \frac{1}{3}(A_{yy} - P^{y'y'})$. Plane wave calculations performed in the impulse approximation predict that at low momentum transfer (q less than 1 fm^{-1}) $A_{yy} = P^{y'y'}$ and $S_2 = 0$ for pure ΔS=0 transitions. For other transitions, $S_2 \approx 0$ and $A_{yy} \approx P^{y'y'}$ are good approximations [13]. We then have $S^y_d \approx S_1$, S^y_d does not depend on tensor polarization measurements and can be written as [12,13]

$$S^y_d = \tfrac{4}{3} + \tfrac{2}{3}A_{yy} - 2K^{y'}_y. \quad (2.2)$$

The only polarization measurement in the focal plane of the spectrometer required to determine S^y_d is the vector-depolarization coefficient $K^{y'}_y$. The only tensor quantity required for S^y_d is A_{yy}, an analyzing power which can be measured easily.

Recently, some of the assumptions used to derive the S^y_d signature have been tested in ^{12}C on the 12.7 MeV, 1^+ state at 4°, with the tensor polarimeter POLDER [17,18]. Within error bars, A_{yy} was found to be equal to $P^{y'y'}$. A value of 0.43 ± 0.05 was measured for the S_1 spin flip probability which is consistent with our present value S^y_d= 0.38 ± 0.03 measured with the vector polarimeter POMME [19,20].

Ishida *et al.* have recently shown that the S_1 probability can be directly obtained for a specific transition via the $(d, d'\gamma)$ reaction, provided the γ-decay branching ratio to the ground state is known [21]. This requirement seriously limits the use of this very nice technique.

A probability for ΔS=1 spin transfer in magnitude (and not in projection like S^y_d) to the deuteron has been derived by Suzuki [22]. However, due to the spin-orbit distortion, it does not always vanish for ΔS=0 transfer to the target. Therefore this observable is not suited for an unambiguous search for ΔS=1 strength in nuclei.

B. Distortion effects

The signature S^y_d has been tested in previous experiments and shown to be generally compatible with zero for natural parity states, while clearly positive for spin transitions. Furthermore, the signature's ability to reliably gauge the presence of isoscalar spin strength in the continuum has been established [13]. It was, however, necessary to check the effects of distortion on all our assumptions and on the signature in particular. The microscopic impulse approximation calculations given in Ref. [13] have been extended to include distortion in both incoming and outgoing channels. The S and D states in the wave function of the deuteron were included. The optical potential parameters used in this paper were obtained by refitting the elastic scattering data of Ref. [23]. These parameters as well as the details of the distorted wave calculations are discussed in Ref. [24] and will be further described in a forthcoming paper. The main results are that in the range of momentum transfers involved in our experiment ($q \leq 1$ fm^{-1}), S_2 is compatible with zero ($S_2 \leq 0.004$) and $A_{yy} \simeq P^{y'y'}$ within a few percent, making S^y_d almost equal to S_1 for all purposes. Distortion effects do not modify significantly the signature S^y_d (at least for $q \leq 1$ fm^{-1}). This is illustrated in Table I, in which the measured values of S^y_d for the natural parity states at 4.44 MeV and 9.64 MeV and for the spin-flip state at 12.7 MeV are compared to the predicted plane wave and distorted wave values. The calculations were done using the Cohen and Kurath [25] wave functions. The measured values for the 4.44 MeV and the 9.64 MeV states are from a previous experiment [13]. The values for the 12.7 MeV state are from the present experiment done with much higher statistics; they are compatible within error bars with our previously published values [12,13].

The differential cross sections, analyzing powers, and spin observables for the 4.44 and 12.7 MeV states are compared to plane wave and distorted wave calculations in Figs. 1 and 2, respectively. The experimental points are from previous experiments [12,23]. The distorted wave calculations (solid lines) generally improve the agreement with the data. The main result is that, in the presence of distortion, the signature S^y_d remains

TABLE I. Signatures for the ΔS=0 states at 4.44 MeV (2^+) and 9.64 MeV (3^-) and, for the ΔS=1 state at 12.7 MeV (1^+) in ^{12}C measured at $\theta = 4°$ and 6°. The theoretical values for S^y_d are calculated using the model of Ref. [24] and the wave functions of Ref. [25].

	Experimental		Plane waves		Distorted waves	
ω (MeV)	4°	6°	4°	6°	4°	6°
4.44	0.03±0.04	-0.01±0.04	0.002	0.004	0.010	0.007
9.64	0.02±0.04	0.03±0.03	0.001	0.002	0.027	0.009
12.71	0.38±0.03	0.30±0.03	0.472	0.299	0.456	0.277

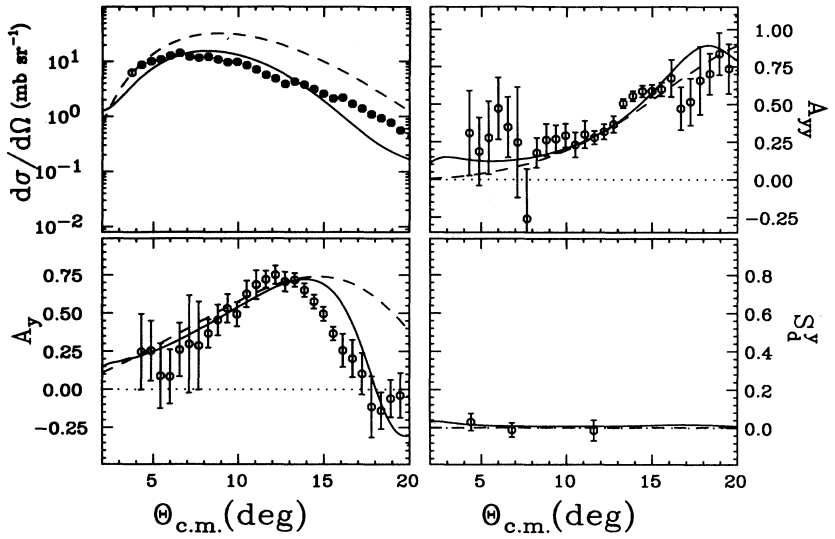

FIG. 1. The measured cross sections, analyzing powers, and S_d^y for the 2^+, 4.44 MeV state are compared to plane wave (dashed line) and distorted wave (solid line) calculations using the CK wave function [25].

close to zero for the 4.44 MeV state and is significantly different from zero for the 12.7 MeV state. One can conclude that S_d^y is indeed a robust signature that remains compatible with zero for ΔS=0 states, while it is clearly positive for spin transitions.

C. Relative spin response

The signature S_d^y is an effective tool for indicating the presence of isoscalar spin strength. For a meaningful study of the ΔT=0 spin response in the continuum, however, a more quantitative variable is needed. For the sake of clarity we will briefly recall some definitions. For a complete derivation and discussion the reader is referred to [13].

Let σ_{00}^A and σ_{10}^A be the isoscalar cross sections for a spin transfer of 0 and 1 to the nucleus. Following the method given in Ref. [26] for $(\vec{p},\vec{p}')$ scattering we can write

$$S_d^y = (\sigma_{10}^A\ \alpha^A)/(\sigma_{00}^A + \sigma_{10}^A), \tag{2.3}$$

where α^A is defined as S_d^y for a pure ΔS=1 transition ($\sigma_{00}^A = 0$).

By making the same approximations as in $(\vec{p},\vec{p}')$ [26], we can replace α^A by α^{free} in free deuteron-nucleon (d-N) scattering and factorize the cross sections as

$$\sigma_{i0}^A = N_{\text{eff}}\ f_{i0}\ \sigma_{i0}^{\text{free}}. \tag{2.4}$$

Here N_{eff} is the effective number of participating nucleons (supposed to be the same in both spin channels), f_{i0} the isoscalar nuclear response in the spin channel i, and $\sigma_{i0}^{\text{free}}$ the d-N scattering cross section calculated for the q value of the deuteron nucleus inelastic scattering in the same spin channel. Then

$$S_d^y = (f_{10}\ \sigma_{10}^{\text{free}}\ \alpha^{\text{free}})/(f_{10}\ \sigma_{10}^{\text{free}} + f_{00}\ \sigma_{00}^{\text{free}}). \tag{2.5}$$

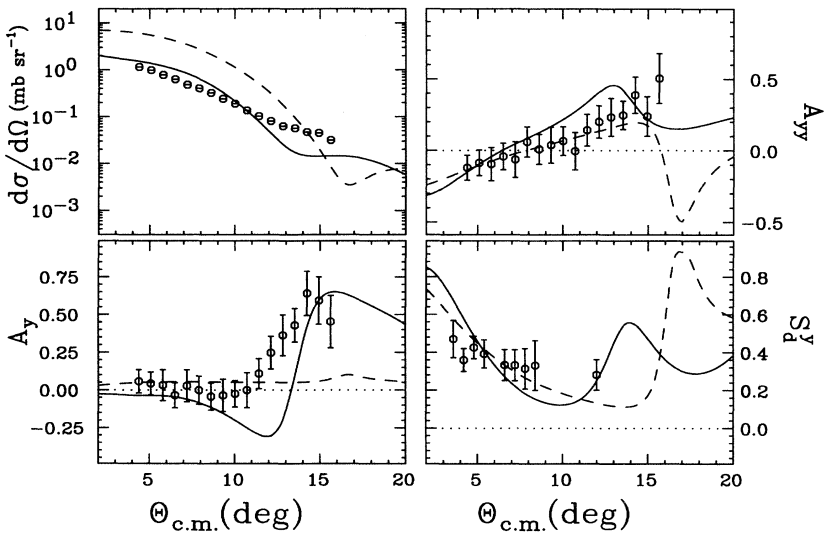

FIG. 2. The measured cross sections, analyzing powers, and S_d^y for the 1^+, 12.7 MeV state are compared to plane wave (dashed line) and distorted wave (solid line) calculations using the CK wave function [25].

The relative isoscalar spin response is defined as

$$R_S^0 = \frac{f_{10}}{f_{10} + f_{00}} \tag{2.6}$$

in analogy with the corresponding isospin-averaged quantity R_S measured in proton scattering.

From the above relations, the ΔS=1 cross section is given by

$$\sigma_{10}^A = \frac{1}{\alpha^{\text{free}}} \frac{d\sigma}{d\Omega} S_d^y(\text{measured}), \tag{2.7}$$

where $\frac{d\sigma}{d\Omega} = \sigma_{00}^A + \sigma_{10}^A$ is the experimental cross section.

It should be noted that if α^{free} is larger than α^A for a particular transition, then the spin cross section σ_{10}^A would be underestimated. The remaining strength would therefore appear as nonspin cross section σ_{00}^A.

III. EXPERIMENTAL SET-UP AND PROCEDURE

The experimental set-up and techniques for this experiment remain essentially the same as described in the ^{40}Ca paper. What follows is a brief review; for a detailed description of the experimental set-up and techniques used to obtain the polarization of the beam and experimental efficiencies the reader is referred to Ref. [13].

The data were taken at the Saturne National Laboratory, using the facility's 400 MeV polarized deuteron beam and the high-resolution magnetic energy-loss spectrometer SPES1 [27]. The polarization of the scattered deuterons was measured with the large focal plane acceptance polarimeter, known by its French acronym POMME. The use of POMME as a vector polarimeter for deuterons is described in detail in [20]. The energy resolution in the focal plane of SPES1 was of the order of 200 keV (FWHM) using a 44 mg/cm^2 ^{12}C target.

The experiment made use of two different modes of beam polarization. In the first mode (the "four-state" mode), the beam is vector and tensor polarized in four different states, the polarization state changing with each beam pulse. In the second mode (the "two-state" mode), the beam is purely vector polarized and alternates between "up" and "down" polarization states. The "four-state" beam was used in order to measure the tensor analyzing power A_{yy} in expression (2.2). Determination of analyzing powers does not require measuring the polarization of the scattered particles, so data were taken rapidly in this phase. When enough data were acquired to determine A_{yy} for each angle and range of excitation energy to be studied, the "four-state" beam was discontinued. The remainder of the experiment was run using the "two-state" mode, which doubled the vector polarization of the incident beam. The intensity of the beam was on the order of 10^{11} deuterons/sec. The vector polarization of the beam p_y was measured regularly and found to be stable within a few percent throughout the whole experiment. The p_y value in the "two-state" mode was equal to 0.611 $\pm$ 0.006, giving a vector polarization efficiency of 91.7%.

Good background rejection was obtained by setting horizontal and vertical windows on target and focal-plane variables of the scattered deuterons. It was shown that, for a deuteron energy of 400 MeV, POMME can cover an excitation energy range of 21 MeV. The systematic error on S_d^y is less than 0.02. The absolute error on the cross sections is estimated to be $\pm$15%.

IV. EXPERIMENTAL RESULTS

Data were taken at spectrometer angles of 4° and 6°. The angular acceptance of SPES1 is 2°, so the entire angular range between 3° and 7° was covered. At each angle, three different, partially overlapping zones of excitation energy were studied, each covering approximately 21 MeV of the focal plane, and centered at 22, 35, and 48 MeV. These data were combined with results from the initial test of S_d^y on ^{12}C on low-lying states to include the entire range of excitation energy up to roughly 58 MeV (q= 0.34 – 0.92 fm^{-1}). The low energy region up to 12 MeV has been extensively discussed in a previous paper [12].

Figure 3 shows the measured missing mass spectra for ^{12}C at 4° and 6°. The natural parity states at 4.44 (2$^+$), 7.65 (0$^+$), and 9.64 (3$^-$) MeV are clearly visible. The 9.64 MeV state is superposed onto the broad 0$^+$ state at 10.3 MeV; the other broad structure at 15.4 MeV is a known 2$^+$ state. Several known isoscalar spin states are also observed in the present experiment. The 1$^+$ state at 12.7 MeV and the 2$^-$ state at 18.3 MeV are among the strongest excited states. The 2$^-$ state at 11.83 MeV is very weakly excited and barely visible in both spectra. The well known 15.1 MeV 1$^+$ state, which is quite prominent in $(\vec{p},\vec{p}')$ spectra at forward angles, is totally absent here due to its isovector nature. Above 20 MeV of excitation energy, several structures, with widths ranging between 1 and 5 MeV, are observed at 20.5, 21.9, 23.8, 25.1, 26.5, 30, and 35 MeV. Most of them are un-

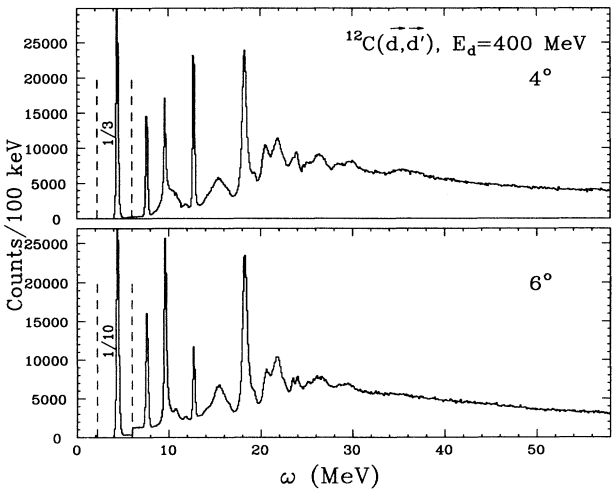

FIG. 3. Missing mass spectra at 4° and 6° (lab) in counts/100 keV.

known if we refer to the most recent published energy levels of ^{12}C [28]. In the tables only one T=0 transition is reported at 21.6 MeV. All of these structures are excited at both angles, except the 5 MeV wide structure at 35 MeV which is seen only in the 4° spectrum. After optimizing background rejection, all of our excitation energy range was virtually background free except the 37–42-MeV region at forward angles, where, in the empty target run, some experimental background (of the order of 5% of the full target counting rate) remained. The empty target measurements are poor in statistics and, although no specific structure was observed at 35 MeV, the present situation does not allow us to ascertain beyond any doubt that the 35 MeV structure observed in the full target runs at forward angles is a real excitation of the ^{12}C nucleus.

The raw missing mass spectra have to be summed in larger size bins in order to get reasonable statistical uncertainties on the calculated signature S_d^y. One chooses the size of the bins in such a way as to have enough statistics in each bin while at the same time preserving as much as possible the shape of the structures. The analysis of the data both with equal size bin and variable size bins leads to the same results. Equal size bins work well for a structureless continuum, but will partially wash out some narrow structures. One has to check the effect of binning on the position and width of narrow structures. This is crucial in particular for the 16–25-MeV region of excitation energy, where a decomposition of the spectrum into different overlapping structures has been carried out. The binned missing mass spectrum at 4° is shown in Fig. 4(a). As a result of the binning, some structures are less visible than in the raw missing mass spectrum.

Figures 4(b) and 4(c), respectively show the signature S_d^y and the response function R_S^0 calculated for each bin

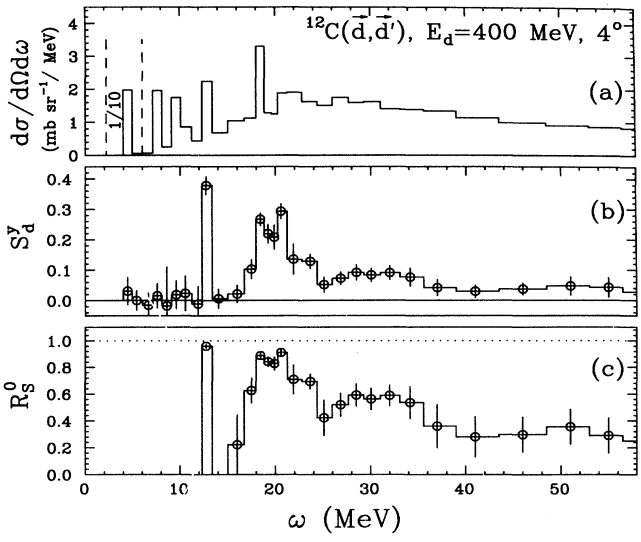

FIG. 4. Results on ^{12}C at 4° (lab) as a function of the excitation energy. (a) The missing mass spectrum binned in energy and normalized to give mb/sr MeV; (b) the signature S_d^y; (c) the relative spin response R_S^0.

across the entire range of excitation energy. The signature for the 12.7 MeV state reaches nearly 0.4, comparable to the values of S_{nn} measured in $(\vec{p},\vec{p}')$ experiments for ΔS=1 states. The signature is also large for the 2^- state at 18.3 MeV and for the 20.5 MeV bin where no isoscalar spin levels are known. The relative isoscalar spin response R_S^0 shows values near unity for the 12.7 MeV (96%) and the 18.3 MeV (90%) states, as expected for pure spin states. The 20.5 MeV bin has a relative spin response of 92%, indicating an almost pure spin state. Below the 12.7 MeV state, the signature is compatible with zero, therefore giving null values of R_S^0 with large error bars. The large errors are due to the fact that small uncertainties in small values of S_d^y lead to large uncertainties in R_S^0, as was shown in Ref. [13]. Therefore the relative spin response is given only for excitation energies above 12 MeV, where it is different from zero.

The 18.3 and 20.5 MeV peaks appear superposed on a broad, resonancelike structure, several MeV in width, and centered around 20 MeV. The relative spin response for this structure is mostly above 70%. In our original paper on ^{12}C [12], a sharp minimum (compatible with zero) was observed in the spin-flip spectrum at 19.8 MeV which led us to conclude that a large structure underneath the 18.3 MeV state was unlikely. The reanalysis of these data [13] with the corrected values of the incident beam polarization and for the POMME analyzing power made this minimum less pronounced and compatible with the presence of a wide structure at 20 MeV, discussed below.

Another much wider concentration of spin strength appears centered near 30 MeV. The signature here is slightly weaker than in the 20 MeV structure and corresponds to a relative spin response of 60%. Beyond the 30 MeV structure, no further significant concentration of spin strength is discernible. The value of S_d^y at higher excitation energies is small and fluctuates around 0.05.

There are more isoscalar spin structures at higher excitation energies than was the case with ^{40}Ca. These structures lead to a relative isoscalar spin response higher than in ^{40}Ca up to $\simeq$35 MeV. Beyond this excitation energy and up to 58 MeV the isoscalar spin response, at 4°, is weaker than in ^{40}Ca for the same domain of excitation energy. The isoscalar spin response R_S^0 never rises above about 0.5 beyond 35 MeV, and thus behaves differently from R_S as determined in $(\vec{p},\vec{p}')$ measurements.

The measured differential cross section (Total) and the deduced nonspin (ΔS=0) and spin (ΔS=1) cross sections at 4° are given in Fig. 5. The spin cross section is compatible with zero below the 12.7 MeV state. The known spin states at 12.7 and 18.3 MeV are clearly seen in the spin cross section. A previously unknown spin state at 20.5 MeV, although partially washed out in the binning of the total cross section, clearly stands out in the spin cross section on top of the 20 MeV bump. The 30 MeV structure is also visible, although less prominently. Above 40 MeV of excitation energy, the spin cross section is very small.

Below 17 MeV of excitation energy, all of the structures in the nonspin cross section correspond to known natural

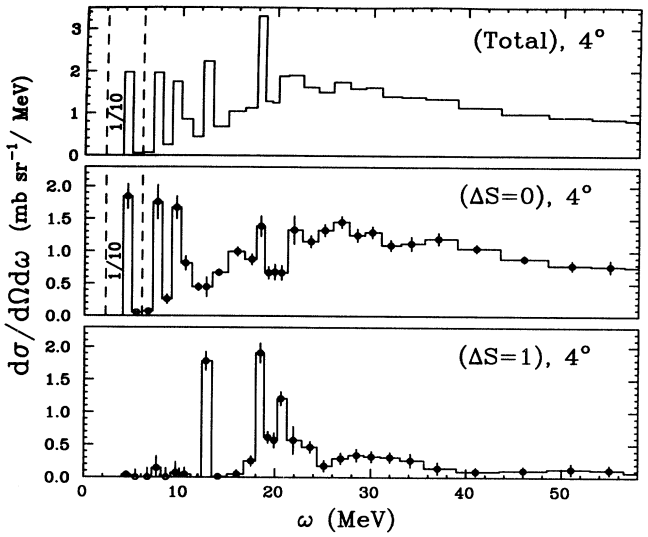

FIG. 5. ΔS=0 and ΔS=1 extracted cross sections (σ_{00} and σ_{10}) compared to the total measured cross section at 4°.

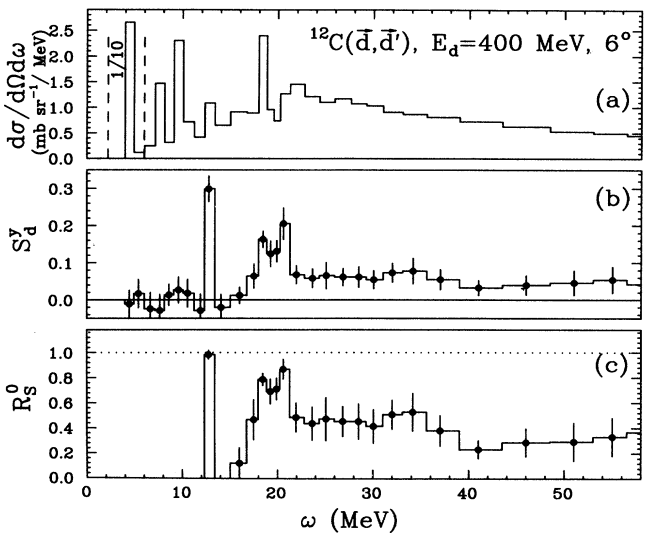

FIG. 6. Results on ^{12}C at 6° (lab) as a function of the excitation energy. (a) The missing mass spectrum binned in energy and normalized to give mb/sr MeV; (b) the signature S_d^y; (c) the relative spin response R_S^0.

parity transitions. Above 18 MeV, only one sharp structure is visible around 18 MeV. This isoscalar ΔS=0 state appears in the binned spectrum at the same excitation energy as the strongly excited 2^- spin state. Following the remark at the end of Sec. II, we calculated the coefficient α^A for the 2^-, T=0 state, using either the Cohen and Kurath wave function [25] or the extended shell model of Unkelbach [29]. For the range of q transfers involved in the present experiment, α^A was found be equal or slightly larger than α^{free}. Based on these results we can say that the existence of this structure is not due to our underestimating the spin cross section for the 2^- state at 18.3 MeV. In the table of energy levels of ^{12}C [28], there is a 3^- (T=1) state at 18.35 MeV which cannot be excited in this experiment and a 3^- (T unknown) at 18.6 MeV. The present data suggests the presence of a $\Delta S = 0$, $T = 0$, and $\Delta L \geq 1$ transition around 18.3 MeV. Clear evidence for a natural parity, likely 2^+, transition at 18.4 ± 0.2 MeV was observed in the inelastic scattering of alpha particles from ^{12}C at 172.5 MeV by Kiss *et al.* [30]. These authors commented that their data appeared inconsistent with the 2^- assignment of Jones *et al.* [31]. Our data suggest that both states are present, and so reconcile the two observations. The ratio of cross sections for the ΔS=0 18.3 MeV state and the 4.44 MeV 2^+ state in (d, d') are roughly consistent with the ratio of (α, α') cross sections seen by Kiss *et al.* In addition, although no ΔS=0 peak was observed near 18.3 MeV in the proton work [14], the ΔS=0 cross section observed in this region with protons is roughly consistent in magnitude and angular distribution with the (α, α') and with the present work.

There is a concentration of ΔS=0 strength between 22 and 36 MeV that cannot be easily separated into individual structures. At comparable momentum transfers, the giant dipole resonance is strongly excited in $(\vec{p}, \vec{p}')$ scattering, and is clearly visible in the nonspin cross section in the region between 17 and 30 MeV. The marked absence of this resonance in the $(\vec{d}, \vec{d}')$ spectrum is consistent with the fact that the GDR is strongly, if not totally, isovector in nature and that the Coulomb excitation of this resonance is negligible. At higher excitation energies, the nonspin cross section is essentially flat and featureless.

The signature and response function for the 6° run are shown in Fig. 6. The behavior of both is largely similar to that of the 4° case, although the wide structures at 20 and 30 MeV are not so clearly resolved. The largest values of S_d^y are still obtained for the states states at 12.7, 18.3, and 20.5 MeV. The measured differential cross section spectrum, together with the deduced nonspin and

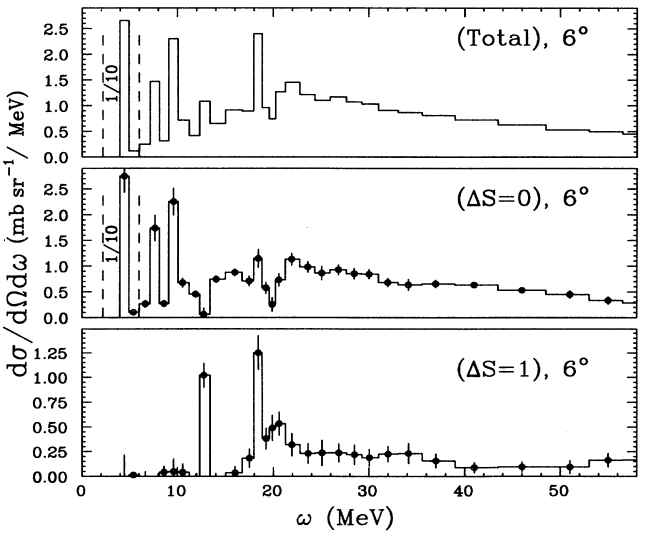

FIG. 7. ΔS=0 and ΔS=1 extracted cross sections (σ_{00} and σ_{10}) compared to the total measured cross section at 6°.

spin cross-section spectra at 6° are given in Fig. 7. In the spin cross-section spectrum, only the 12.7 and the 18.3 MeV peaks are clearly visible. The 20.5 MeV peak has strongly decreased and is barely visible on top of the 20 MeV structure. The nonspin cross-section spectrum is essentially identical to the 4° spectrum. The isoscalar ΔS=0 state at 18 MeV is clearly seen and the concentration of ΔS=0 strength between 20 and 36 MeV is slightly more pronounced than at 4°.

The 16–25-MeV region where narrow and large structures overlap has been binned in equal size steps of 500 keV. In order to take into account the effect of the position of the bins with respect to the raw spectrum we have generated five histograms by each time shifting the bins by 100 keV. By overlapping in the same figure (Fig. 8) all the generated histograms represented with different symbols, one can see the effect of the position of the bins on the width and shape of the structures. One clearly sees two sharp peaks at 18.3 and 20.5 MeV on top of a broad structure. The decomposition of this region was carried out assuming Gaussian shaped peaks. In order to see if our present data are compatible with the observation by Bland *et al.* in forward angle pion scattering [32] of a 3 MeV wide spin structure at 20 MeV, we have forced our fit to have a broad structure (at least 3 MeV wide) centered at 20 MeV. The best fit obtained at 4° is shown as a continuous line in Fig. 8; the dashed line represents the individual structures that the fit has found. The result of our best fit obtained at different angles clearly shows the existence of the 20.5 MeV state with a width equal to that of the 18.3 MeV state. Furthermore, our data are compatible with the excitation of a 3 MeV wide structure at 20 MeV. More structures are needed in order to fit the spectrum, especially between 22 and 25 MeV. However from the present data, one can confidently give spin cross sections only for the two narrow structures and the remaining strength integrated between 16 and 25 MeV.

The angular distributions for the different structures observed in the spin cross-section spectra are presented in Fig. 9. For the 12.7 and 18.3 MeV levels, the measured

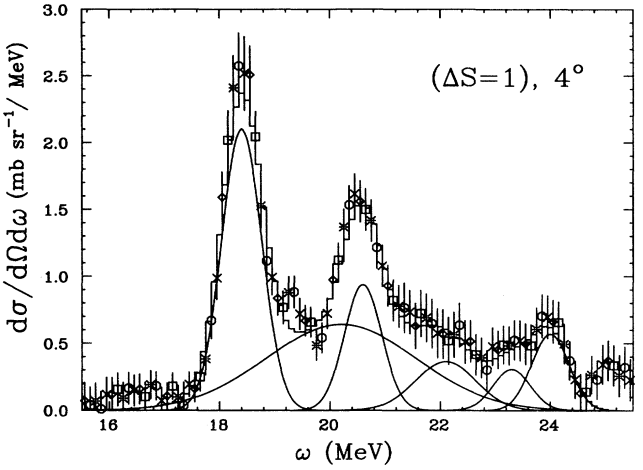

FIG. 8. The ΔS=1 binned spectrum at 4° between 16 and 25 MeV of excitation energy. The decomposition into individual structures is shown as the dashed line histogram. The solid line represents the best fit to the total spectrum. For the different symbols in the histogram, see text.

differential cross sections are compared to our recent microscopic DWIA calculations [24]. The dashed (solid) curve represents the plane (distorted) wave calculations using the wave functions of Ref. [25]. The distorted wave calculations substantially improve the agreement with the measured cross sections. It should be stressed that no normalization coefficient is used in the present calculations. For the 12.7 MeV state, the distorted wave calculation still overpredicts the differential cross section by 50%. The sharp T=0 spin state at 20.5 MeV has a forward peaked angular distribution slightly steeper than that of the 12.7 MeV state. Nevertheless, the shape of the calculated angular distribution for the 12.7 MeV state (dotted curve) reproduces quite well the measured angular distribution of the 20.5 MeV state, suggesting a 1^+ assignment.

The integrated spin strength between 16 and 25 MeV (minus the cross sections for the 18.3 and 20.5 MeV

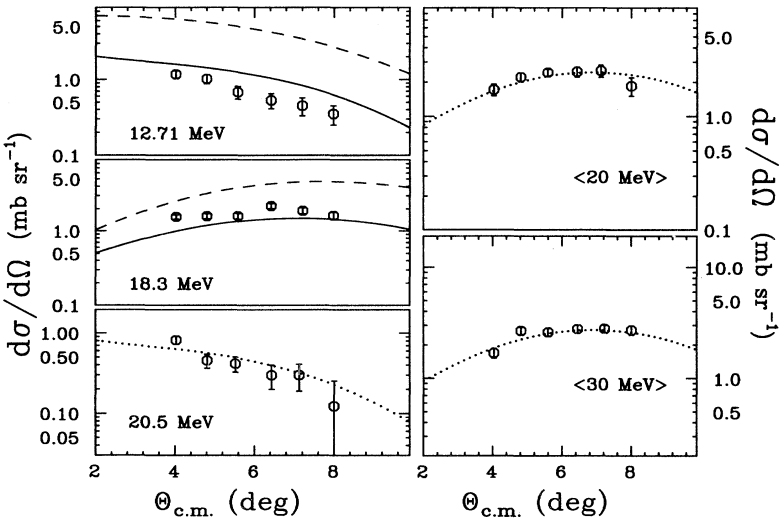

FIG. 9. Angular distributions of spin cross section σ_{10} for the three narrow ΔS=1 states at 12.7 MeV (known 1^+), 18.3 MeV (known 2^-), and 20.5 MeV (new 1^+) and the two large structures centered at 20 and 30 MeV. The theoretical curves are described in the text.

states) and between 25 and 35 MeV, are, respectively, labeled ⟨20 MeV⟩ and ⟨30 MeV⟩. The measured angular distributions of the differential cross sections for ⟨20 MeV⟩ and ⟨30 MeV⟩ have a slight maximum around 6°. The limited angular range and the poor statistics which result from smaller angular bins do not allow definitive multipolarities to be extracted. Nonetheless, the shapes of the angular distributions are close to that of the 18.3 MeV level (dotted curve) and therefore compatible with ΔL=1 transitions. The ⟨20 MeV⟩ region thus seems to contain the ΔL=1, ΔS=1, ΔT=0 resonance previously suggested in (π,π') [32], which appears to be the isoscalar component of the spin dipole resonance. The centroid of the spin dipole resonance is observed around 22 MeV in $(\vec{p},\vec{p}')$ [14] and at 22.7 MeV in backward angle electron scattering experiments [33], which are sensitive primarily to the isovector components.

Using the 318 MeV $(\vec{p},\vec{p}')$ results of Ref. [14], the spin-isospin response ratios were generated for ^{12}C as they were for ^{40}Ca in Ref. [13]. These ratios were calculated only for a limited range of excitation energies because no $(\vec{p},\vec{p}')$ data are available above 43 MeV. The behavior of these ratios can be seen in Fig. 10 and is very similar to that of ^{40}Ca. The concentration of mainly L=1 isoscalar spin strength close to 20 MeV clearly appears in the ratio f_{10}/f_{00}. In the same region of excitation energy a cluster of isovector spin strength appears in the ratio f_{11}/f_{00}. Beyond 20 MeV of excitation energy, the behavior of all three ratios is strongly reminiscent of the response ratios of ^{40}Ca, steadily increasing for (f_{11}/f_{00}), and steadily decreasing for (f_{10}/f_{11}). More ΔS=1, ΔT=1 strength appears at high excitation energy than ΔS=1, ΔT=0 strength and beyond about 25 MeV the isovector spin strength dominates.

V. SUMMARY AND CONCLUSIONS

The ^{12}C $(\vec{d},\vec{d}')$ studies have yielded several interesting results. The ΔS=1 state at 18.3 MeV, dominated by the $(1d_{5/2}, 1p_{3/2}^{-1})$ transition in the Cohen-Kurath description, has been identified as a J^π=2$^-$ spin-flip isoscalar state in $(\vec{p},\vec{p}')$ experiments [31]. The present results confirm this designation. Data from inelastic pion and electron scattering [34] experiments have also identified 2$^-$ strength in this region. Of course if the 18.3 MeV state were purely isoscalar in nature, it would scarcely be noticeable in electron scattering, but the results appear consistent with the isospin mixing measured in the pion studies [31]. In the nonspin cross-section spectra, a state of similar width is observed around 18 MeV. It appears that this state corresponds to a 2$^+$ state at 18.4 MeV observed clearly in 172.5 MeV alpha scattering by Kiss *et al.* [30]. It suggests that two states of the same total spin and opposite parity overlap near 18 MeV.

A relatively sharp peak is observed in the spin cross section near 20.5 MeV. This previously unknown state has been tentatively identified as an isoscalar (1$^+$) spin state. Comparison of the data for this state with theoretical expectations is currently being pursued.

The concentration of ΔT=0 spin strength near 20 MeV is compatible with the approximately 3 MeV wide spin structure observed in forward angle pion scattering and identified there as the 1$^-$ component of the spin dipole resonance [32].

An additional broad structure at 30 MeV contains substantial spin strength (R_S^0 of the order of 60–70 %) with an angular distribution compatible with ΔL=1. Little significant structure was observed in the spin-flip cross section at higher energies. The signature S_d^y was roughly consistent with its free value for excitation energies above 35 MeV.

The enhancement of R_S at high excitation energies that was observed in proton scattering has no analog in $(\vec{d},\vec{d}')$, where R_S^0 fluctuates below its Fermi-gas value of 0.5. The lack of enhancement of R_S^0 in the continuum (as previously observed in ^{40}Ca) is consistent with a weakly repulsive residual particle-hole interaction in the S = 1, T = 0 channel. Theoretical predictions for the value of

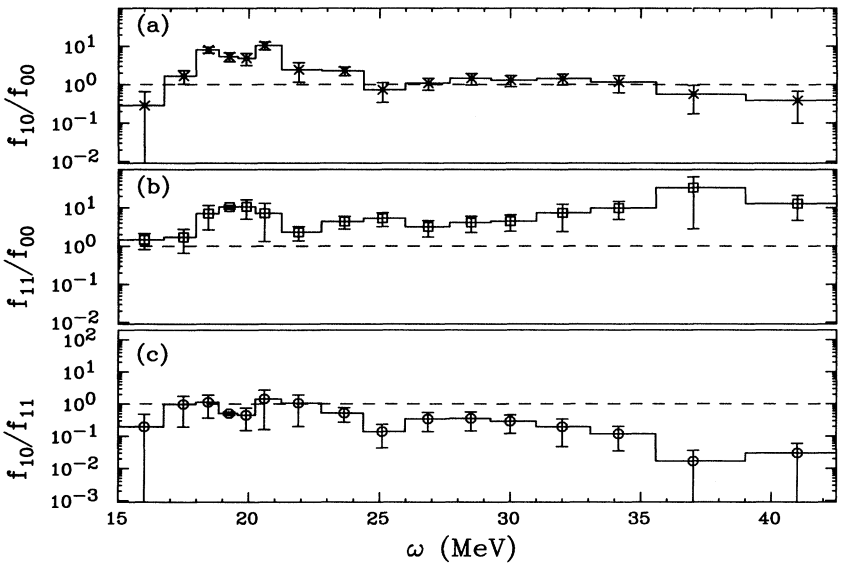

FIG. 10. Relative spin strengths. (a) f_{10}/f_{00} extracted from the present $(\vec{d},\vec{d}')$ data; (b) f_{11}/f_{00} obtained using the relative spin responses R_S^0 (present data) and R_S ($(\vec{p},\vec{p}')$ at 318 MeV); (c) f_{10}/f_{11} ratio of the ΔT=0 to the ΔT=1 strength in the spin channel.

the Landau-Migdal parameter g_0 vary widely. Simple π- and ρ-meson exchange models, for example, predict a rough parity between g_0 and g_0' [35]. Although some theorists have used weak repulsion in this channel [36], the lack of any experimental constraint provided no incentive to assume a weakly repulsive residual interaction. The present results together with the ^{40}Ca results are consistent with the conclusions previously deduced from the observation of the dominantly isoscalar spin state at 5.845 MeV in ^{208}Pb [37]. Experimental evidence is growing in favor of a weakly repulsive residual particle-hole interaction in the $S = 1$, $T = 0$ channel.

Preliminary microscopic DWIA calculations are compared to PWIA calculations and show substantial improvement in the agreement with measured cross sections and analyzing powers. The details of these calculations will be given in a forthcoming paper. The most important result is that the signature S_d^y remains a good signature even in the presence of distortion.

ACKNOWLEDGMENTS

We are grateful to the technical staff of the Laboratoire National Saturne for its efficient assistance during the experiment. We would like to thank Y. Bisson, G. Chesneau, and R. Margaria for their help during the setup of the experiment. Some of the authors (B.N.J., C.D., F.T.B., and C.G.) were supported by grants from the National Science Foundation and the U.S. Department of Energy.

[1] J. Rapaport, T. Taddeucci, T. P. Welch, C. Gaarde, J. Larsen, D. J. Horen, E. Sugarbaker, P. Koncz, C. C. Foster, C. D. Goodman, C. A. Goulding, and T. Masterson, Nucl. Phys. **A410**, 371 (1983).

[2] J. Rapaport, R. Alarcon, B. A. Brown, C. Gaarde, J. Larsen, C. D. Goodman, C. C. Foster, D. Horen, T. Masterson, E. Sugarbaker, and T. N. Taddeucci, Nucl. Phys. **A427**, 332 (1984).

[3] J. Watson, B. D. Anderson, and R. Madey, Can. J. Phys. **65**, 566 (1987).

[4] A. Brockstedt, L. Berqgvist, L. Carlen, P. Ekström, B. Jakobsson, C. Ellegaard, C. Gaarde, J. S. Larsen, C. D. Goodman, M. Bedjidian, D. Contardo, J. Y. Grossiord, A. Guichard, J. R. Pizzi, D. Bachelier, J. L. Boyard, T. Hennino, J. C. Jourdain, M. Roy-Stéphan, M. Boivin, T. Hasegawa, and P. Radvanyi, Nucl. Phys. **A530**, 571 (1991).

[5] A. Richter, in *Proceedings of the International Conference on Nuclear Physics*, Firenze, Italy, 1983, edited by P. Blasi and R. A. Ricci (Tipografia Compositori Bologna, 1984), p. 189.

[6] C. Djalali, N. Marty, M. Morlet, A. Willis, J. C. Jourdain, A. Anantaraman, G. M. Crawley, and A. Galonsky, Nucl. Phys. **A388**, 1 (1982).

[7] C. Djalali, These d'état, Université Paris XI, Orsay, 1984.

[8] F. T. Baker, L. Bimbot, R. W. Fergerson, C. Glashausser, K. W. Jones, A. Green, K. Nakayama, and S. Nanda, Phys. Rev. C **37**, 1350 (1988).

[9] F. T. Baker, L. Bimbot, R. W. Fergerson, C. Glashausser, A. Green, K. Jones, W. G. Love, and S. Nanda, Phys. Rev. C **40**, 1877 (1989).

[10] O. Häusser, M. C. Vetterli, R. W. Fergerson, C. Glashausser, R. G. Jeppesen, R. D. Smith, R. Abegg, F. T. Baker, A. Celler, R. L. Helmer, R. Henderson, K. Hicks, M. J. Iqbal, K. P. Jackson, K. W. Jones, J. Lisantti, J. Mildenberger, C. A. Miller, R. S. Sawafta, and S. Yen, Phys. Rev. C **43**, 230 (1991).

[11] F. T. Baker, L. Bimbot, R. W. Fergerson, C. Glashausser, A. Green, O. Häusser, K. Hicks, K. W. Jones, C. A. Miller, M. C. Vetterli, R. Abegg, D. Beatty, B. Bonin, B. Castel, X. Y. Chen, V. Cupps, C. Djalali, R. Henderson, K. P. Jackson, R. G. Jeppesen, K. Nakayama, S. K. Nanda, R. S. Sawafta, and S. Yen, Phys. Rev. C **44**, 93 (1991).

[12] M. Morlet, A. Willis, J. Van de Wiele, N. Marty, J. Guillot, H. Langevin-Joliot, L. Bimbot, L. Rosier, E. Tomasi-Gustafsson, G. W. R. Edwards, R. W. Fergerson, C. Glashausser, D. Beatty, A. Green, C. Djalali, F. T. Baker, and J. C. Duchazeaubeneix, Phys. Lett. B **247**, 228 (1990).

[13] M. Morlet, E. Tomasi-Gustafsson, A. Willis, J. Van de Wiele, N. Marty, C. Glashausser, B. N. Johnson, F. T. Baker, D. Beatty, L. Bimbot, C. Djalali, G. W. R. Edwards, A. Green, J. Guillot, F. Jourdan, H. Langevin-Joliot, L. Rosier, and M. Y. Youn, Phys. Rev. C **46**, 1008 (1993).

[14] F. T. Baker, D. Beatty, L. Bimbot, V. Cupps, C. Djalali, R. W. Fergerson, C. Glashausser, G. Graw, A. Green, K. W. Jones, M. Morlet, S. K. Nanda, A. Sethi, B. H. Storm, W. Unkelbach, and A. Willis, Phys. Rev. C **48**, 1106 (1993).

[15] *Proceedings Third International Symposium on Polarization Phenomena in Nuclear Reactions* (Univ. of Wisconsin Press, Madison, WI, 1971).

[16] G. G. Ohlsen, Rep. Prog. Phys. **35**, 717 (1972).

[17] J. S. Real, Ph.D. thesis, 1994 University of Grenoble (unpublished).

[18] S. Kox, C. Furget, J. S. Real, L. Bimbot, J. P. Bocquet, M. Garçon, C. Djalali, C. W. R. Edwards, C. Glashausser, B. N. Johnson, M. Morlet, C. Perrin, D. Rebreyend, L. Rosier, E. Tomasi-Gustafsson, E. Voutier, and A. Willis, Nucl. Instrum. Methods Res. Sec. A **346**, 527 (1994).

[19] B. Bonin, A. Boudard, H. Fanet, R. W. Fergerson, M. Garçon, C. Giorgetti, J. Habault, J. Le Meur, R. M. Lombard, J. C. Lugol, B. Mayer, J. P. Mouly, E. Tomasi-Gustafsson, J. C. Duchazeaubeneix, J. Yonnet, M. Morlet, J. Van de Wiele, A. Willis, G. Greeniaus, G. Gaillard, P. Markowitz, C. F. Perdrisat, R. Abegg, and D. A. Hutcheon, Nucl. Instrum. Methods Phys. Res. Sec. A **288**, 379 (1990).

[20] B. Bonin, A. Boudard, H. Fanet, R. W. Fergerson, M. Garçon, C. Giorgetti, J. Habault, J. Le Meur, R. M. Lombard, J. C. Lugol, B. Mayer, J. P. Mouly, E. Tomasi-Gustafsson, J. C. Duchazeaubeneix, J. Yonnet, M. Morlet, J. Van de Wiele, A. Willis, G. Greeniaus, G. Gaillard, P. Markowitz, C. F. Perdrisat, R. Abegg, and D. A. Hutcheon, Nucl. Instrum. Methods Phys. Res.

Sec. A **288**, 389 (1990).
[21] S. Ishida, H. Sakai, H. Okamura, H. Otsu, N. Sakamoto, K. Hatanaka, and A. Okihana, Phys. Lett. B **314**, 279 (1993).
[22] T. Suzuki, Prog. Theor. Phys. **86**, 1129 (1991).
[23] T. Mandon, Ph.D thesis, Université Paris XI, Orsay, 1991.
[24] J. Van de Wiele, A. Willis, M. Morlet, and E. Tomasi-Gustafsson, IPN-Orsay Internal Report IPNO/Ph/94-11, 1994.
[25] S. Cohen and D. Kurath, Nucl. Phys. **73**, 1 (1965); K. W. Jones Ph.D. thesis, Rutgers University, 1984 (Los Alamos Laboratory National Laboratory Report No. LA-10064-T, 1984) (unpublished).
[26] C. Glashausser, K. W. Jones, F. T. Baker, L. Bimbot, H. Esbensen, R. W. Fergerson, A. Green, S. Nanda, and R. D. Smith, Phys. Rev. Lett. **58**, 2404 (1987).
[27] R. Beurtey, *Summer School, Nuclear and Particle Physics at Intermediate Energies*, Brentwood College School, B.C., Canada, 1975; J. Saudinos, J. C. Duchazeaubeneix, C. Laspalles, and R. Chaminade, Nucl. Instrum. Methods **11**, 77 (1973).
[28] F. Ajzenberg-Selove, Nucl. Phys. **A506**, 1 (1990).
[29] W. Unkelbach, private communication.
[30] A. Kiss, C. Mayer-Boricke, M. Rogge, P. Turek, and S. Wiktor, J. Phys. G **13**, 1067 (1987).
[31] K. W. Jones, C. Glashausser, S. Nanda, R. de Swiniarski, T. A. Carey, W. Cornelius, J. M. Moss, J. B. McClelland, S. J. Seestrom-Morris, J. R. Comfort, J.-L. Escudie, M. Gazzaly, N. Hintz, G. Igo, M. Haji-Saeid, and C. A. Whitten, Phys. Lett. **128B**, 281 (1983).
[32] L. C. Bland, R. Gilman, G. S. Stephans, G. P. Gilfoyle, H. T. Fortune, C. L. Morris, S. J. Seestrom-Morris, S. J. Greene, P. A. Seidl, R. R. Kiziah, and C. F. Moore, Phys. Lett. **144B**, 328 (1984).
[33] A. Yamagushi, T. Terasawa, K. Nakahara, and Y. Torizuka, Phys. Rev. C **3**, 1750 (1971).
[34] C. L. Morris, *Workshop on Nuclear Structure with Intermediate Energy Probes*, LNAL Report No. LA-8303-C, 1980 (unpublished).
[35] G. E. Brown, S.-O. Backman, E. Oset, and W. Weise, Nucl. Phys. **A286**, 191 (1977).
[36] T. S. Dumitrescu and T. Suzuki, Nucl. Phys. **A423**, 277 (1984).
[37] H. Toki, G. F. Bertsch, and D. Cha, Phys. Rev. C **28**, 1398 (1983).